LINEAR ATTENUATION COEFFICIENT OF SOIL SAMPLES IN NWE NYEIN REGION BY USING GAMMA ENERGY AT 662 keV

Aye Aye Mar[1] and Khin Mya Mon[2]

Abstract

The linear attenuation coefficients μ of two types of soil samples collected from different areas in Nwe Nyein village, Shwebo Township, Sagaing region have been determined by using gamma radiation at energy 662 keV for different soil samples. Firstly we collected two types of soil samples. And then each sample is made dry and ground to get powder. A cylindrical container of 6cm diameter is used to measure gamma penetrating for three different thicknesses of 1cm, 2cm and 3cm. The results have been presented in a graphical form. The increasing linear nature of graphs of number of particles of radiation counted without absorber (Io) per number of particles of radiation counted with absorber (I) *vs* the thickness of absorber are fitted by the least square method. According to the values of the linear attenuation coefficients, the soil sample R1 is the most suitable for the 662keV gamma ray shielding.

Key words: gamma-ray spectrometry, environmental samples, linear attenuation coefficients

Introduction

The attenuation coefficient is an important parameter, which is widely used in industry, agriculture, science, and technology, *etc*. The properties characterizing the penetration and diffusion of gamma rays in composite materials such as soil are very important. Soil has chemical properties as on its compositions and has physical properties. Gamma-ray spectrometry is one of the most widely used techniques to determine the linear attenuation coefficient of soil samples. In order to obtain correct results the samples should be counted under the same measuring conditions as those under which the system has been calibrated.

[1] Assistant Lecturer, Dr., Department of Physics, University of Mandalay

[2] Professor and Head, Dr., Department of Physics, University of Mandalay

Attenuation of Gamma Rays

In gamma rays spectroscopy, one is most commonly interested only in the fraction of the monoenergetic photons that have been penetrated the layer without any interaction and therefore has their original energy and direction. The term "attenuation" refers to the remaining photons that have either been absorbed or scattered in the layer.

Linear Attenuation Coefficient

When gamma rays transverse a small thickness of matter dx at any point in a medium, the extents of the photons are proportional to the radiation intensity and the thickness transverse at that point. Consequently, in transverse the distance dx, the intensity of the gamma rays photons which have not undergone interaction will be decreased by

$$dI = -\mu I dx$$

$$\frac{dI}{I} = -\mu dx$$

Where, I is the intensity, e.g., in photons per cm^2 per second, and μ is the proportionality constant, usually expressed in cm^{-1} unit. All three types of interaction of gamma-rays photons with matter are included.

Each of the interaction processes removes the gamma rays photon from the beam either by absorption or by scattering away from the detector direction, and can be characterized by a fixed proper ability of occurrence per unit length in absorber. The sum of this proper ability of occurrence per unit path length that the gamma rays photon is removed from the beam.

$$\mu = \mu\,(\text{photoelectric}) + \mu\,(\text{compton}) + \mu\,(\text{pair})$$

Where, μis called the linear attenuation coefficient of the absorber for the given radiation. If a collimated (parallel) beam of monoenergetic gamma rays of intensity I_0 passes through a thickness x of absorber, the intensity I of the emerging photons which have not suffered any interaction is obtained by integration of equation, the result is

$$\ln I/I_0 = -\mu x$$

$$I = I_o \exp(-\mu x)$$

Where, μ = linear attenuation coefficient of the medium

I = intensity of gamma rays

I_0= initial intensity of gamma radiation

x = thickness of absorbing material

EXPERIMENTAL SETUP AND PROCEDURE

Gamma Spectroscopy System

A gamma spectroscopy system consists of a detector, electronics to collect and process the signals produced by the detector, and a computer with processing software to generate the spectrum and display and store it for

analysis. Gamma spectroscopy detectors are passive materials that wait for a gamma interaction to occur in the detector volume. The most important interaction mechanisms are the Photoelectric effect, the Compton Effect, and Pair production. The photoelectric effect is preferred, as it absorbs all of the energy of the incident gamma rays. Full energy absorption is also possible when a series of these interaction mechanisms take place within the detector volume. When a gamma ray undergoes a Compton interaction or Pair Production, and a portion of the energy escapes from the detector volume without being absorbed, the background rate in the spectrum is increased by one count. This count will appear in a channel below the channel that corresponds to the full energy of the gamma rays. Larger detector volumes reduce this effect. The voltage pulse produced by the detector (or by the photomultiplier in a scintillation detector) is shaped by a multichannel analyzer (MCA). The multichannel analyzer takes the very small voltage signal produced by the detector, reshapes it into a Gaussian or trapezoidal shape, and converts it into a digital signal.

In some systems, the analog to digital conversion is performed before the peak is reshaped. The analog to digital converter (ADC) also sorts the pulses by their height. ADCs have specific numbers of "bins" to sort the pulses into; these are the "channels" in the spectrum. The number of channels can be changed in most modern gamma spectroscopy system by changing a software or hardware setting. The number of bins is a power of two. Common values include 512, 1024, 2048, 4096, 8192, or 16384 channels. The choice of number of channels depends on the resolution of the system and the energy range being studied. The MCA output is sent to a computer which stores, displays, and analyzes the data. A variety of software packages are available from several manufacturers, and generally include spectrum analysis tools such as energy calibration, peak area and net area calculation, and resolution calculation. Other components, such as rate meters and peak position stabilizers, may also be included.

The present gamma spectroscopy system includes the following components. They are Na (Tℓ) scintillation detector associated with ORTEC (Model 296) photo multiplier tube, high voltage power supply, pre amplifier (Model 142 PC), amplifier (Model 671) and a pulse stored multi-channel analyzer (MCA) together with gamma vision 32 software installed in PC. The high voltage power supply was used for supplying the potentials for the detector. The operating voltage for NaI (Tℓ) scintillation detector is 800V. The 3"x 3" NaI (Tℓ) scintillation detector was used to detect the gamma radiation intensity before and after passing through the absorbing material and this information (electronic pulses) were amplified and stored in MCA based on personal computer [5].

Energy Calibration

The energy of radioactive elements in soil sample is unknown. The standard radioactive sources of known energies were used to calibrate the spectrometer. Therefore, energy calibration was first made for 300 seconds by using ^{60}Co (1173.23 keV), ^{137}Cs (661.66 keV) and ^{241}Am (60 keV) sources. In this work, conversion gain is set at 2048. And then sources were placed on the detector surface and a spectrum was accumulated for times period long enough

to determine the peak position. The amplifier gain and shaping time were adjusted until peaks were obtained at the desired energy.

A ^{60}Co source is convenient because its two peaks at 1173 keV and 1332 keV are close energy for ^{40}K (1460 keV). Establishing a direct relationship between photo peak energy and multi channel analyzer channel number can do the energy calibration process. In doing so, energy calibration curve was obtained. Energy calibration data is listed in Table 1 and energy calibration curve is shown in Fig1.

Table1 Energy Calibration Data

Sources	Channel Number	Energy (keV)
^{241}Am	68	60
^{137}Cs	661.93	662
^{60}Co	1143.67	1173
^{60}Co	1319	1332

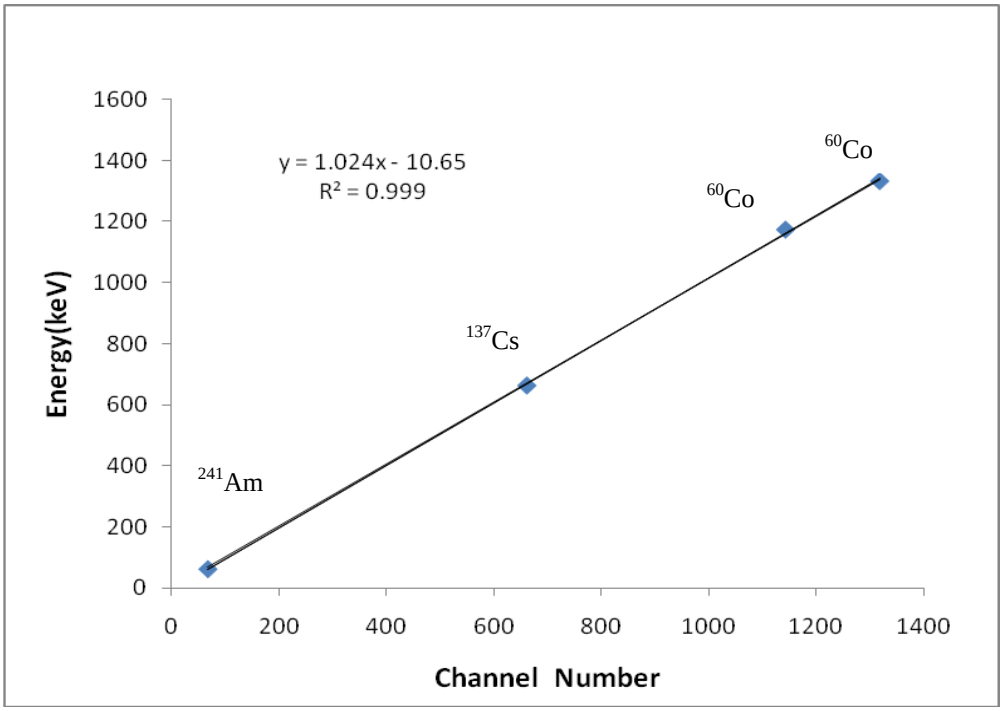

Fig. 1 Energy Calibration Curve

Sample Collection and Preparation

Two soil samples are collected from different places of NweNyein village, Shwebo township, Sagaing region. There are two different types of soil samples; red soil samples (R1, R2, R3 and R4) and yellow soil samples from the places which produce clay (Y1, Y2, Y3 and Y4). Each sample is cleaned by removing unwanted material by meshes and ground to get powder. Then, each sample is sieved with 120 meshes (0.21 mm).

Experimental Procedure

The NaI (Tℓ) gamma detection system was shown in Fig. 2. In gamma-rays spectroscopy system the following equipments are included. They are sodium crystal mounted a photomultiplier tube, preamplifier, amplifier, a pulse sorter (MCA), high-voltage power supply and data readout devices.

In this experiment, NaI(Tℓ) 3" × 3" scintillation detector was used to detect the gamma radiation after passing through the absorbing material and these passed information (electron pulses) were amplified by preamplifier and the fast spectroscopy amplifier and collected by using MCA based on personal computer. The scintillation detector used in operating voltage is 800 V. This value is fixed for all measurements and measuring time in 300 seconds. The experimental set up used in this investigation is shown in Fig 3. In the present work, gamma source ^{137}Cs was used. ^{137}Cs has activity of 1μCi and half-life of 30.1 yrs. Firstly the ^{137}Cs standard source without absorber is placed 10 cm in front of NaI crystal. The corresponding equipments are systematically prepared and connected all over are switch-on. Then the emitted-variations from the source are detected by the NaI (Tℓ) detector and a spectrum is stored for a period of 300 seconds. After these, standard source is positioned at the centre of the container. In this experiment, the gamma source, a detector and sample container are placed as shown in Fig. 3.4.The gamma rays line of 662 keV was resolved with the help of the scintillation detector. The transmitted intensity through the soil sample thickness can be calculated by using the equation 1.7 and 1.8.

The incident beam intensity and the attenuated beam intensity were measured to calculate the attenuation coefficient of soil. The source positioned at the centre of the sample and detector was taken to be optimum. The collected data and spectrum for each measurement is stored and analyzed by using Gamma Vision 32 software. The spectra were marked for ROI and the gross counts, net count of full energy peak were collected. By using the net count of gamma rays spectra of soil samples, the net intensity rate is plotted against the sample thickness. The values of linear attenuation coefficient (μ) were obtained by using Equation 1.6.

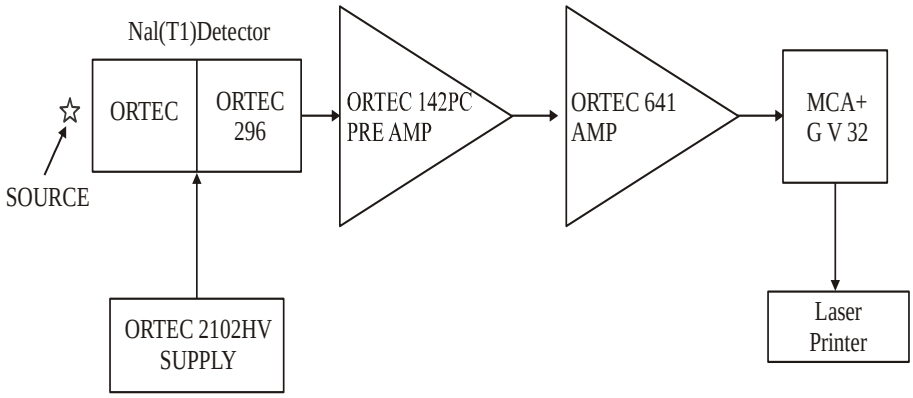

Fig. 2 NaI (Tℓ) Detection System

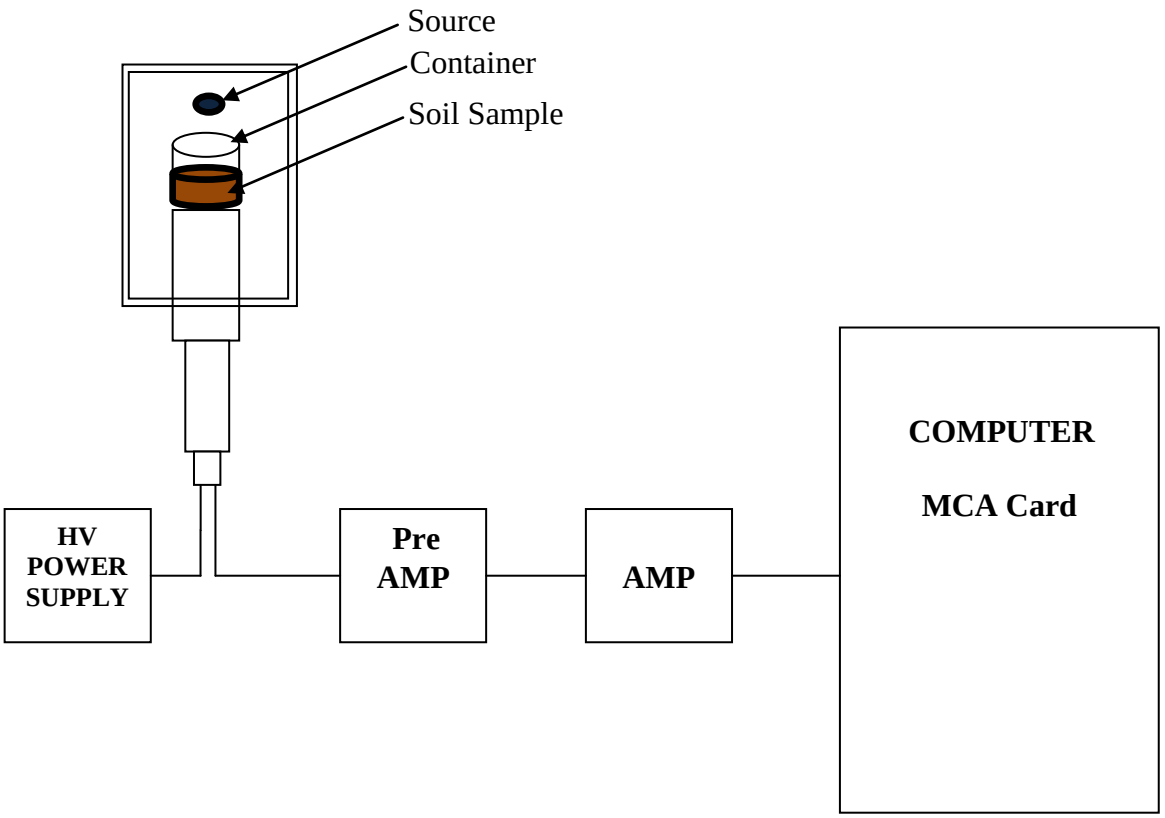

Fig. 3 Experimental Set-up of measuring system

solar voltage, converted voltage of the charging current and the reference voltage are applied to the microcontroller unit.

PIC16F877A microcontroller is used as the main control device and it performs the required ADC functions and mathematical calculations. The DC voltage regulator unit provides regulated +5V for this section. The measured values are displayed by means of a 20-character 4-line LCD module. The constructed system can measure the solar charging current, solar charging voltage, solar panel open circuit voltage (V_{OC}), solar panel short circuit current (I_{SC}), instantaneous output power of solar panel and maximum power value for a day.

Solar Panel Tracking Section

Block diagram and complete circuit diagram of solar panel tracking section is shown in Figure 3. and Figure 4. respectively.

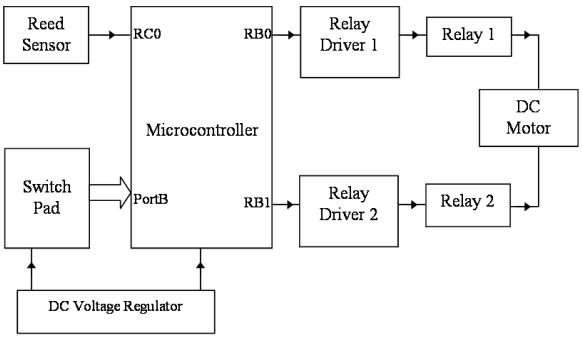

Figure 3. Block diagram of solar panel tracking section

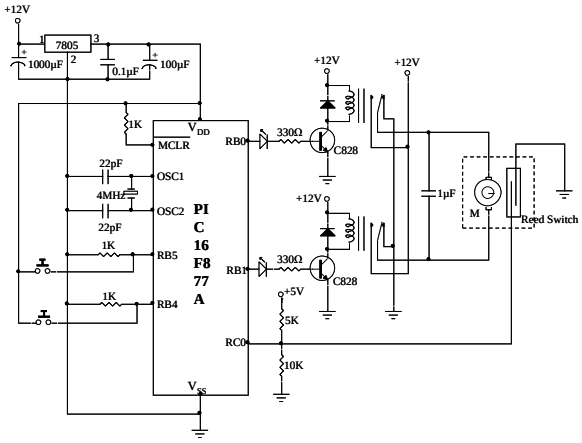

Figure 4. Complete circuit diagram of solar panel tracking section

The reed switch is employed to sense the rotation of DC motor and it generates the pulses when the motor rotates in any direction. These pulses are fed to the built-in counter unit of microcontroller and the microcontroller calculates the movement of solar panel using incoming pulses. The control signals for motor operations (bidirectional rotations and stopping) are generated from the microcontroller after calculating the kinematics variables

based on the instant position of the panel and kinematics parameters of the mathematical structure of the frame.

The two button switches are also installed to adjust the orientation of solar panel manually. In order to power the DC motor, two relays are used in this circuit and these relays are energized via the relay driver unit composing NPN transistors. The constructed system applied a DC motor for the single-axis control and it is intended to achieve the constant angular speed of solar panel. The panel is driven to move for one degree at each instance of driving and then waits for nearly 4.4 minutes (260 seconds) delays. About 136 degrees and 25200 seconds delay are used for a day (from 9:00 to 4:00).

Kinematics of Tracking System

Kinematics is one of the important fields in Physics. Kinematics deals with motion only, especially for geometry of motion. Solving the kinematics model of a system is essential for any control systems. In this research work, the solar panel is placed on a solar tracking frame and controlled to enhance the output power. Figure 5. shows the photograph of solar panel tracking system. Figure 6. depicts the kinematics model of solar panel tracking system.

Figure 5. Photograph of solar panel tracking system

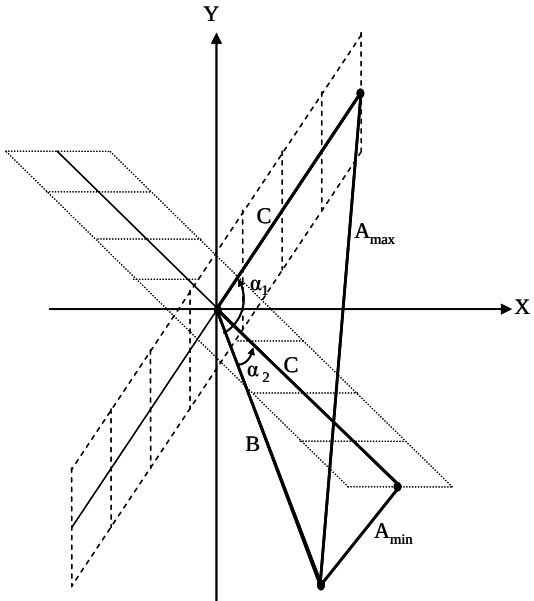

Figure 6. Kinematics model of solar panel tracking system

In Figure 6., the lengths of B and C are constant parameters and the measurements are 29cm and 27cm respectively. But the measurement of A is variable and it can be obtained

indirectly from the total number of pulses coming from reed switch. The maximum length of A (A_{max}) causes the largest angle α_1 and the minimum length of A (A_{min}) gives the smallest angle α_2. The values of angle α are calculated from the measurement of the length of A by applying the law of cosine. The equation for the tracking frame can be written as follows.

(1)

The angle can be redefined as in the following equation.

$$\alpha = \cos^{-1}\left(\frac{B^2 + C^2 - A^2}{2BC}\right) \qquad (2)$$

The above two equations can describe the position and orientation of the solar panel. The measurements of A_{max} and A_{min} are 52 cm and 8 cm respectively for our frame. So, the largest angle α_1 is 136° and the smallest angle α_2 is 16°.

Control Programs

The performance of solar power measuring section is controlled by an embedded microcontroller and also the performance of solar panel tracking section is controlled by another embedded microcontroller. The program source codes of these control programs are composed of data acquisition subroutines, calibration subroutines, LCD control subroutines, data communication macro and 32-bit mathematical subroutines. Figure 7. shows the flowchart of control program for solar power measuring section. The flowchart of control program for solar panel tracking section is described in Figure 8.

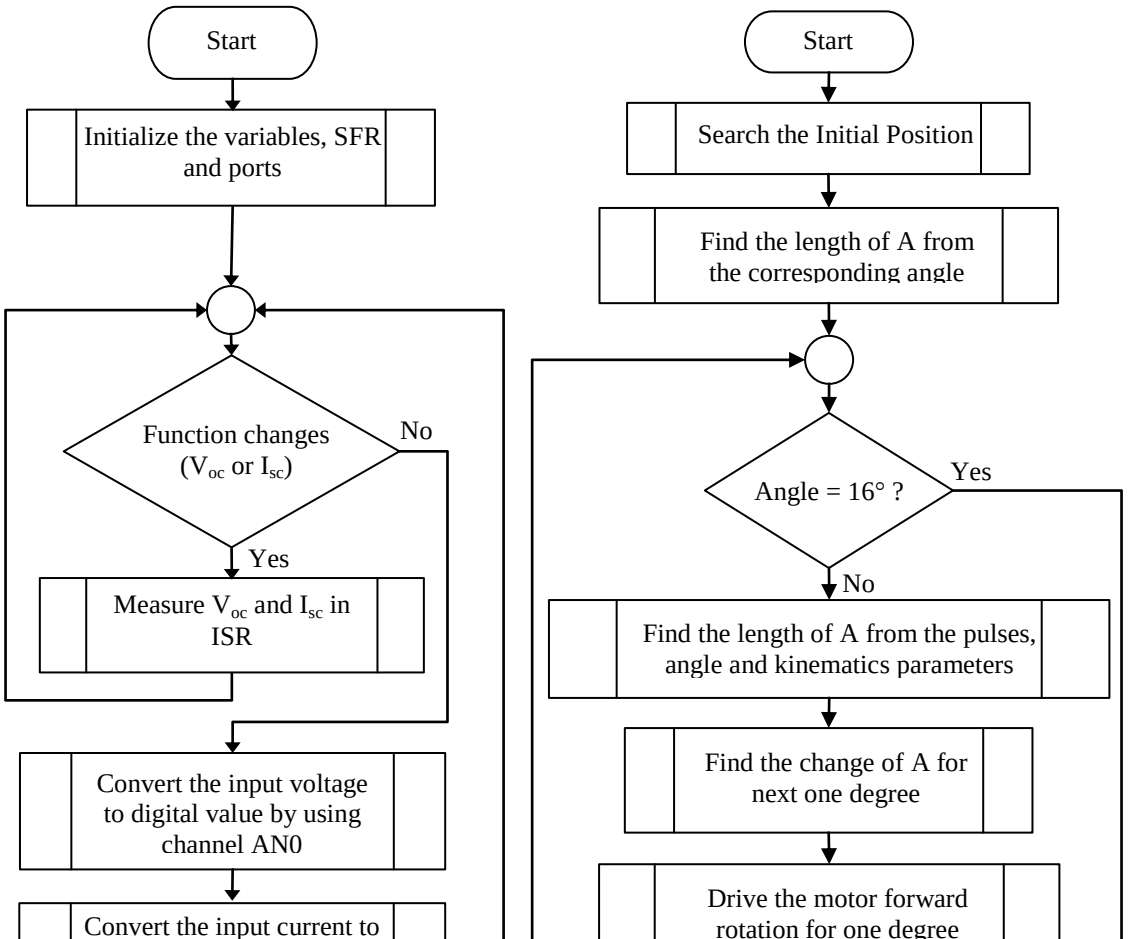

Figure 7. Flowchart of control program for solar power measuring section

Figure 8. Flowchart of control program for solar panel tracking section

Results and Discussions

A microcontroller-based solar panel power measuring system has been designed and constructed. The constructed system can measure the instantaneous power (P_t) and the maximum power (P_m) of the solar panel. The measurable range is from 0W to 500W for power measuring and the resolution is 0.1W. The power measurement is based on the current and voltage measurement. The constructed system can measure also the open circuit voltage (V_{oc}) and the short circuit current (I_{sc}) of the solar panel. The measurable ranges are from 0 A to 10 A for current measuring and from 0 V to 50 V for voltage measuring. The resolutions are 0.01 A for current measuring and 0.01 V for voltage measuring. The solar panel power measuring section of the constructed system is calibrated by using the digital multi-meter (ME 540) as the standard device.

The constructed system was used in data collection for solar energy utilization research work conducted at Department of Physics, University of Mandalay. The charging voltage, current and power versus time graphs are drawn using collected data. Figure 9. shows the charging voltage values for a day without tracking. In Figure 10., the charging voltage values are plotted with local time of a day with solar panel tracking. It is found that the charging voltage is reduced about 3V due to line resistance (1.4Ω). The load (battery) voltage gradually increases when it becomes charge full. The solar panel output voltage shows this characteristics when the panel tracking is used. However, the solar panel output voltage gradually decreases if the tracking section is not used.

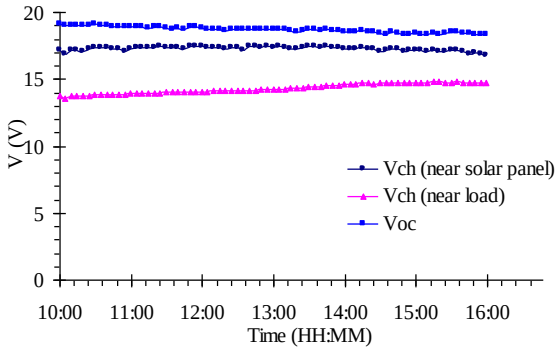

Figure 9. Voltage versus time graph without tracking

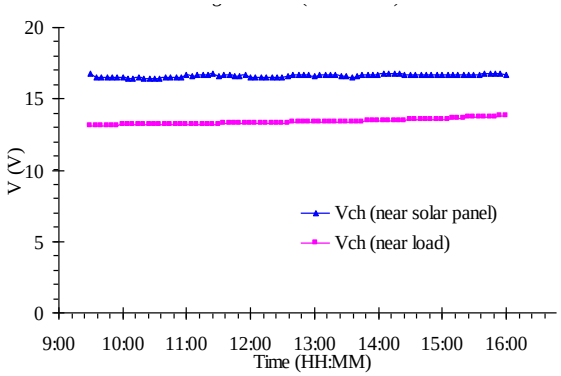

Figure 10. Voltage versus time graph with tracking

The open circuit voltage (V_{oc}) and the short circuit current (I_{sc}) are important parameters for analyzing the performance of the solar cell. In this research work, also V_{oc} and I_{sc} are measured for two cases, with and without tracking. The open circuit voltage is generally constant values in the whole day. While system works without tracking, I_{sc} values are smaller in the evening than those with tracking. The maximum values of the short circuit current are found to be got at around 12:00. The current versus local time graphs are shown in Figure 11. and Figure 12. for two cases, without and with tracking.

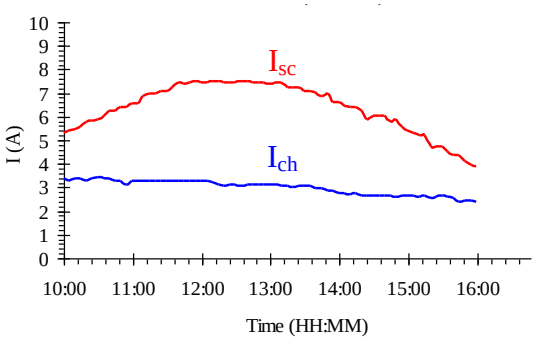

Figure 11. Current versus time graph without tracking

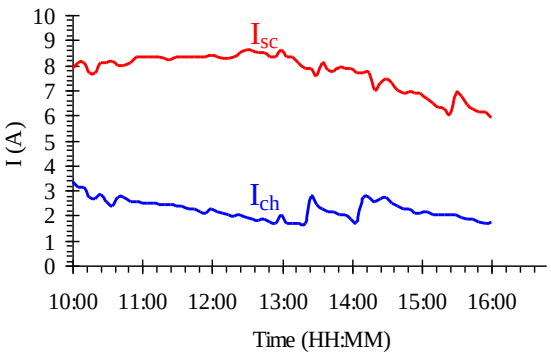

Figure 12. Current versus time graph with tracking

The measured voltage and current values are used to obtain the power. The power is calculated by using 32-bit mathematical subroutines. The measured voltage, current and power displayed on a 20-character 4-line LCD module. According to the experimental data, it is found that the fluctuations occur at the charging power due to weather condition and load.

Figure 13. shows the charging power of the solar panel versus time graph without tracking and Figure 14. expresses the charging power of the solar panel versus time graph with tracking.

Figure 13. Power versus time graph without tracking

Figure 14. Power versus time graph with tracking

In those figures, the upper graph line represents the output power of solar panel and the lower one gives the power values measured on the load (battery). The power at load is smaller than that of panel because of line resistance (1.4Ω). The output power of the solar panel significantly decreases at evening if the tracking is not used. The output power is found to be near 40W for the whole day of operation with tracking. Some of the tracking designs are constant speed tracking method, light sensing control method, maximum power point tracking method. Constant speed control method is used in present system. This method follows the sun constantly in a day whether the weather is fine or not. Hence, this tracking method overcomes the malfunctioning which occurs in light sensing control method.

Conclusion

This research has presented the construction of a constant angular speed solar panel tracking system and solar panel power measuring by using embedded microcontrollers. Specifically, this research expresses a software based working solution for maximum solar panel output by positioning a solar panel. The constructed system can measure the solar charging current, charging voltage and instantaneous output power. So it is expected to be an essential part of an advanced solar energy utilization system. The presently constructed system can be modified for data logging purpose by using EEPROM. One of the modern solar panel control methods is maximum power point tracking method (MPPT) and the instantaneous maximum power value is the control variable of such control method. Our goal is to design and construct an MPPT system and it will be implemented in the near future.

Acknowledgements

The authors are thankful to Dr Mya Aye, Rector, University of Mandalay, for his permission and encouragement to conduct this research work. We would like to express our gratitude to Dr Khin Swe Myint, Pro-rector, University of Mandalay, for her invaluable suggestions. We also thank to Professor Dr Htun Hlaing, Department of Physics, University of Mandalay, for his valuable technical advice.

References

Fisk, M.J., and Anderson, H.C.W., (1982). *Introduction to Solar Technology*, Addison-Wesley Publishing Company, Inc., United States of America.

Iovine, J., (2000). *PIC Microcontroller project book*. McGraw-Hill Book Company, United State of America.

Pradash, J., and Garg, H.P., (2006). *Solar Energy Fundamentals and Applications*. Tata McGraw-Hill Company, India.